CALCULATION METHODS OF INTERACTION OF ELECTROMAGNETIC WAVES WITH OBJECTS OF COMPLEX GEOMETRIES

MYKOLA SHOPA

Gdansk University of technology
Narutowicza 11/12, 80-233 Gdansk, Poland

Abstract: Modeling of the electromagnetic interaction with different homogeneous or inhomogeneous objects is a fundamental and important problem. It is relatively easy to solve Maxwell equations analytically when the scattering object is spherical or cylindrical, for example. However, when it loses these properties all that is left for us is to use approximation models, to acquire the solution we need. Modeling of complex, non-spherical, asymmetric particles is used to study cosmic, cometary dust, aerosols, atmospheric pollution etc. Few analytical, surface-based and volume-based methods of light scattering modeling, most commonly used by scientists, are reviewed here.

Keywords: Light scattering, Mie theory, Direct dipole approximation, Finite Difference time domain method, T-matrix

1. Introduction

Light scattering theories are widely used to model light interaction with arbitrary particles. As mentioned they can be used to study cosmic and cometary dust, aerosols, but also to analyze optical particle counters such as phase Doppler anemometry (PDA), visibility- or intensity-based counters, laser diffraction instruments and light extinction instruments. Scattering computations help in understanding new physical phenomena or in designing new particle diagnostics systems for the identification of variations in particle optical properties or the particle shape.

Furthermore, computation of light scattering by particles plays an enormous role in optical particle sizing, astronomy, optical oceanography, photographic science, meteorology and coatings technology. Similar electromagnetic modeling methods are needed to investigate microwave scattering by raindrops and ice

crystals or to analyze electromagnetic interference problems. A number of light scattering theories have been developed and extensive overviews of available theories have been published in multiple papers [1–3]. Reviews on related subjects of nanooptics and metamaterials have been published by Myroshnychenko *et al.* [4] and by Veselago *et al.* [5].

Methods of light scattering modeling can be split into three categories. Analytical methods, which are based on a separation of the variables approach, surface-based methods, where the boundary conditions are enforced on the surface of the scattering particle and only this surface is discretized, and volume-based methods, where the volume of the particle and, with some methods, also φ part of the surrounding medium is discretized.

Mie theory is restricted to spherical, homogeneous, isotropic and non-magnetic particles in a non-absorbing medium. Mie scattering is an important tool for diagnosing micro particles or aerosol particles in technical or natural environments. However, as micro particles are hardly ever spherical or homogeneous, this theory is limited in use. Extension of Mie theory covers coated spheres, stratified spheres and clustered spheres. For homogeneous non-spherical particles such as spheroids, ellipsoids and finite cylinders, surface discretization methods have been developed. Scattering by inhomogeneous particles may be computed by volume discretization methods. During recent decades, scattering methods for non-spherical and non-homogeneous particles have been developed and multiple computer codes are readily available.

2. Mie theory

In 1908 Gustav Mie presented his universal solutions describing light scattering on spherical, nonmagnetic particles [6–8]. He assumed that homogeneous, isotropic, nonmagnetic, spherical particle was illuminated by a plane, linearly polarized monochromatic wave along the x-axis. Maxwell's equations with the divergent free electric field $\nabla \cdot \boldsymbol{E} = 0$ are the starting points of the description with the constitutive relations and the continuity relations at the sphere boundary. In such case, the harmonic solutions $\boldsymbol{E}(\boldsymbol{r},t) = \boldsymbol{E}(\boldsymbol{r})e^{-i\omega t}$ and $\boldsymbol{H}(\boldsymbol{r},t) = \boldsymbol{H}(\boldsymbol{r})e^{-i\omega t}$ for the electric and magnetic field outside and inside the particle must satisfy the homogeneous wave equations.

The electric and magnetic fields outside the sphere in a nonconducting, nonmagnetic medium are assumed to be a superposition of incident fields and scattered by the sphere fields:

$$
\begin{aligned}
\boldsymbol{E}_{\text{out}} &= \boldsymbol{E}_{\text{inc}} + \boldsymbol{E}_{\text{scat}} \\
\boldsymbol{H}_{\text{out}} &= \boldsymbol{H}_{\text{inc}} + \boldsymbol{H}_{\text{scat}}
\end{aligned}
\tag{1}
$$

The incident plane wave as well as the scattered and internal fields are expanded into spherical vector wave functions in spherical polar coordinates (r, θ, φ). Solu-

tions of the vector wave equation can be written in form of a sum of vectors of spherical harmonics $\boldsymbol{M}_l$ and $\boldsymbol{N}_l$ [8]:

$$\boldsymbol{M}_l = \nabla \times (\boldsymbol{r}\psi_l)$$
$$k\boldsymbol{N}_l = \nabla \times \boldsymbol{M}_l \tag{2}$$

where ψ_l denotes generating functions that satisfy the scalar wave equation in spherical coordinates (3):

$$\nabla^2 \psi_l + k^2 \psi_l = 0 \tag{3}$$

The appropriate generating functions are used to expand the incident plane wave (linearly polarized along x-axis) into a series of vector harmonics and to express the electric $\boldsymbol{E}_{\text{inc}}$ and magnetic $\boldsymbol{H}_{\text{inc}}$ field as a linear superpositions of these harmonics. The same scalar functions are used to expand the electric $\boldsymbol{E}_{\text{in}}$ and magnetic $\boldsymbol{H}_{\text{in}}$ fields inside the sphere. Another scalar solution of (3) corresponding to the outgoing wave in its radial part is used to construct a vector solution for the scattered electric $\boldsymbol{E}_{\text{scat}}$ and magnetic $\boldsymbol{H}_{\text{scat}}$ fields with coefficients a_l and b_l of the expansion. The expansion coefficients of the scattered field can be found by enforcing the boundary condition on the spherical surface. In particular, coefficients a_l and b_l take the following form:

$$a_l = -\frac{j_l(mx)\big[xj_l(x)\big]' - \big[mxj_l(mx)\big]'j_l(x)}{j_l(mx)\big[xh_l^{(1)}(x)\big]' - \big[mxj_l(mx)\big]'h_l^{(1)}(x)} \tag{4}$$

$$b_l = -\frac{m^2 j_l(mx)\big[xj_l(x)\big]' - \big[mxj_l(mx)\big]'j_l(x)}{m^2 j_l(mx)\big[xh_l^{(1)}(x)\big]' - \big[mxj_l(mx)\big]'h_l^{(1)}(x)} \tag{5}$$

where:

$$x = \frac{2\pi n_{\text{out}} R}{\lambda} \qquad m = \frac{n_{\text{in}}}{n_{\text{out}}} \tag{6}$$

x is the size parameter, m – the relative refraction index of the particle, R – the particle radius, λ – the vacuum wavelength of the incident light, $n_{\text{in}} = \sqrt{\mu_{\text{in}}\varepsilon_{\text{in}}}$ – the particle refractive index, $n_{\text{out}} = \sqrt{\mu_{\text{out}}\varepsilon_{\text{out}}}$ – the surrounding medium refractive index. To simplify the coefficients (4)–(5) we can replace the Bessel j_l and Hankel $h_l^{(1)}$ functions by the Rikkati–Bessel functions:

$$\psi_l(x) = xj_l(x)$$
$$\xi_l(x) = xh_l^{(1)}(x) \tag{7}$$

It has been demonstrated that Mie theory can be now successfully applied up to size parameters of 10,000 [9–11].

As Mie theory is restricted to spherical homogeneous spheres, there are many extensions of this theory covering different aspects. A scattering theory for magnetic spheres can easily be formulated, what can be relevant for scattering at infrared or microwave frequencies.

Many advanced algorithms have been developed over recent decades, the scattering theory of coated dielectric spheres algorithm [12], an algorithm for a sphere having two coatings [13]. This was used to compute the internal field of

a particle at resonance. The differential light scattering patterns of single bacterial spores were measured [14]. This pattern was matched to theoretical patterns computed by a core shell model. In this way the inner and outer refractive indices and the inner and integument thickness of the spore were found.

Another derivation from a Mie sphere is a slightly non-spherical particle. This may be treated by a first-order perturbation approach. In this case the assumptions are that the particle is homogeneous and that the deviations from sphericity are small and smooth, such as a droplet distorted by a fluid flow. There is also an extension of Mie theory to an anisotropic spherical shell which is an appropriate model to study light scattering by a variety of biological systems.

A further extension of Mie theory which is of great interest in optical particle sizing is scattering of a sphere excited by a laser beam having a Gaussian intensity distribution. The beam may be expanded into spherical vector wave functions by computing beam shape coefficients in the framework of the generalized Lorenz-Mie theory (GLMT) or into a spectrum of plane waves. Different methods to compute the beam shape coefficients have been developed. A rigorous approach is based on surface integration. The coefficients of a Gaussian beam can also be computed by a finite series for on-axis particle positions. The localized approximation of the beam shape coefficients leads to the fastest algorithm. This method can also be applied to computation of the morphological resonances induced by off-axis illumination of a sphere by a focused laser beam. The GLMT has recently been adapted to shaped beam scattering by a coated sphere and a multi layered sphere.

For nanosized noble metal particles of size lower than about 20 nm, various modifications, extensions and corrections to Mie's original theory are needed to take into account that "sharp" boundary conditions do not hold in the nanoscale [15]. The author used modified Mie theory to model surface plasmons resonances on the surface of Au nano- and mesosized particles (Figure 1), [16]. Kreibig in [17] lists also complementary models to the Mie theory, an incident wave not plane, a non step-like boundary condition, dielectric function dependent on the particle size. These extensions help to explain the measured absorption spectra of Ag nanoparticles and plasmon polaritons.

Until recently, it was the Mie theory which was mainly applied to analyze optical particles. However, as particles of interest are hardly ever spherical or homogeneous, there is much interest in more advanced scattering theories that are not that much restricted. In recent decades, scattering theories of non-spherical and inhomogeneous particles have been developed greatly, mostly because of the growth of the computational capabilities of modern computers.

3. T-matrix

The coefficients of the scattered field f_{mn}, g_{mn} are related to the coefficients of the incident field a_{mn}, b_{mn} by the transition matrix or just T-matrix. The transmitted and scattered incident field is expanded into a series of spherical
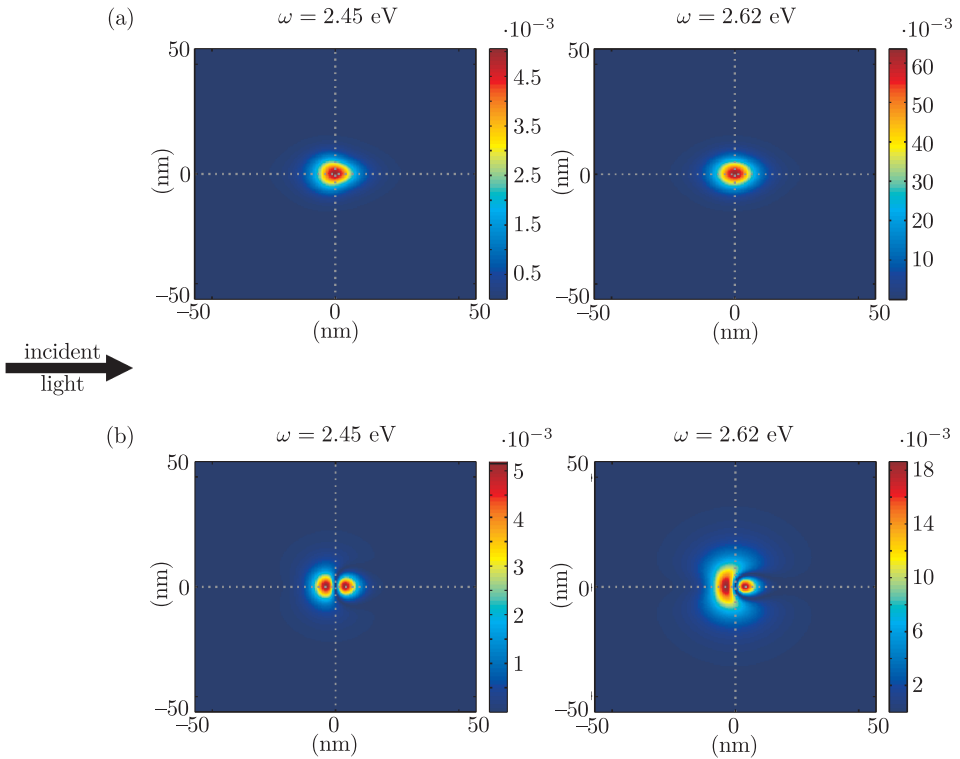
Figure 1. Numerical images at scanning plane placed at the close proximity of the particle surface: distance to the sphere surface in the center of image $d = 0$, radius of the sphere $R = 10$ nm; the frequency of incident light ω is off resonance and equal to the dipole surface plasmon resonance frequency at $\omega_{\mathrm{res}} = 2.62$ eV (a) polarization parallel to the scanning plane l_{Hh} (a.u.) ($l = 1\ldots 3$), (b) polarization perpendicular to the scanning plane l_{Vv} (a.u.) ($l = 1\ldots 3$)

vector wave functions. These functions are fundamental solutions of the vector Helmholtz equation and can be generated from the scalar fundamental solutions in spherical coordinates, the spherical Bessel functions of the first kind and the spherical Hankel Functions. Accordingly, there are two linearly independent sets of solutions denoted as $\boldsymbol{M}^1$, $\boldsymbol{N}^1$ and $\boldsymbol{M}^3$, $\boldsymbol{N}^3$, respectively.

$$\boldsymbol{E}_{\mathrm{inc}} = \sum_{n=1}^{\infty} \sum_{m=-n}^{n} a_{mn} \boldsymbol{M}_{mn}^1 + b_{mn} \boldsymbol{N}_{mn}^1 \tag{8}$$

$$\boldsymbol{E}_{\mathrm{scat}} = \sum_{n=1}^{\infty} \sum_{m=-n}^{n} f_{mn} \boldsymbol{M}_{mn}^3 + g_{mn} \boldsymbol{N}_{mn}^3 \tag{9}$$

$$\begin{pmatrix} a_{mn} \\ b_{mn} \end{pmatrix} = T \begin{pmatrix} f_{mn} \\ g_{mn} \end{pmatrix} \tag{10}$$

The T-matrix elements can be obtained by numerical integration. For an arbitrarily shaped particle a surface integral has to be computed, which is computationally expensive. Most implementations of the methods are restricted

to axisymmetric scatterers, as in this case line integrals have to be computed. It is easy to extend the T-matrix method to coated spheroids. For example, this allows to model water-coated ice particles in the atmosphere. An incident Gaussian beam profile can also be included in the theory. Recent improvements make the method applicable to particles with size parameters well exceeding 100. The advantage of this method is that the T-matrix is computed, which includes a full solution of the scattering problem [18–20].

4. Finite Difference Time Domain Method

The finite difference time domain (FDTD) method is an electromagnetic modeling technique which is very popular in electrodynamics. With the FDTD method an entire volume including the scatterer is discretized. It is very suitable for scattering computations of non-spherical and inhomogeneous particles. The basic element of this discretization is the Yee cell [21]. The Yee cell (Figure 2) is the basic element of an interlocked grid with the electric field E representing an unknown on the edges of one grid and the magnetic field H representing the unknowns on the faces of the grid. The differential form of Maxwell's equations is solved directly. A difference approximation is applied to evaluate the space and time derivatives of the field. The time step is denoted by Δt and the grid spacing by Δx, Δy, Δz. μ is the magnetic permeability.

$$H_{x(ijk)}^{n+1/2} = H_{x(ijk)}^{n-1/2} + \frac{\Delta t}{\mu \Delta z}\Big(E_{y(ijk)}^{n} - E_{y(ijk-1)}^{n}\Big) - \frac{\Delta t}{\mu \Delta y}\Big(E_{z(ijk)}^{n} - E_{z(ij-1k)}^{n}\Big) \quad (11)$$
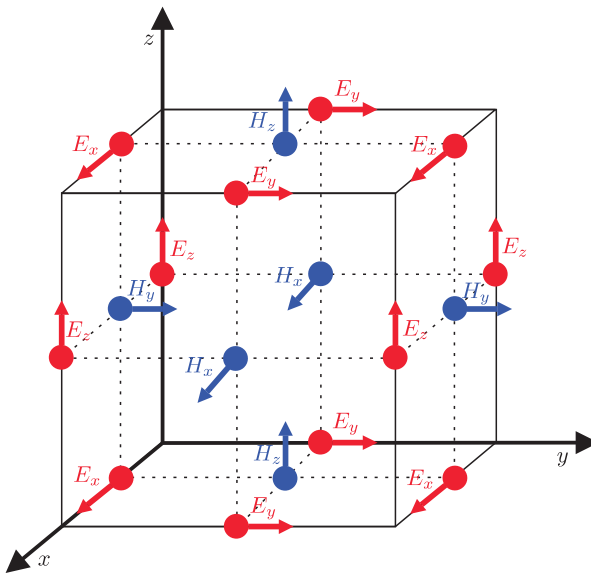

Figure 2. Yee cell with labeled electric and magnetic field components

A similar difference equation is used to find the unknown electric field from the magnetic field. By alternating these two computations at each time step,

the field propagates through the whole volume. This time marching scheme is applied until a steady-state solution is obtained. Each grid point of the volume may have different values of permittivity so that an inhomogeneous scatterer can be computed. Special absorbing boundary conditions are needed for simulation of scattering such that the wave is not reflected at the open boundary of the discretized volume. A near-field to far-field transformation is needed to compute the scattered far-field from the near-field values of the computational volume. The grid distance has to be smaller than the incident wavelength.

The FDTD is a time-domain technique, and when a broadband pulse (such as a Gaussian pulse) is used as the source, then the response of the system over a wide range of frequencies can be obtained with a single simulation. This is useful in applications where resonant frequencies are not exactly known, or anytime that a broadband result is desired. Since the FDTD calculates the electric and magnetic fields everywhere in the computational domain as they evolve in time, it provides animated displays of the electromagnetic field movement through the model that helps to ensure that the model is working correctly.

The FDTD allows the effects of apertures to be determined directly. Shielding effects can be found, and the fields both inside and outside a structure can be found directly or indirectly.

Nonetheless, since the FDTD requires that the entire computational domain be gridded, and the grid spatial discretization must be sufficiently fine to resolve both the smallest electromagnetic wavelength and the smallest geometrical feature in the model, very large computational domains can be developed, which results in very long solution times. Models with long, thin features, (like wires) are difficult to model in the FDTD due to an excessively large computational domain required. Another weakness of this method is that there is no way to determine unique values for permittivity and permeability at a material interface. Space and time steps have to satisfy the CFL condition, or the leapfrog integration used to solve the partial differential equation is probable to become unstable. The computational domain has to be finite to permit its residence in the computer memory. This can be achieved by inserting artificial boundaries into the simulation space. Most FDTD implementations use a special absorbing "material", called a perfectly matched layer (PML) to implement absorbing boundaries. Grosge *et al.* [22] compared numerical scattering results in context of near-field spectroscopy for the FDTD on gold nanostructures where the geometrical singularities at the edges of the square generate a high gradient of the electric near field.

There are multiple commercial FDTD software vendors [23, 5, 24] as well as a number of open source FDTD development projects [25–28].

5. Direct Dipole Approximation

The direct-dipole approximation (DDA) also known as discrete-dipole approximation is a powerful technique for computing scattering and absorption by objects of arbitrary geometry. The basic idea of the DDA was introduced in 1964

by DeVoe, [29, 30] who applied it to study the optical properties of molecular aggregates. The DDA, including retardation effects, was proposed in 1973 by Purcell and Pennypacker, [31] who used it to study interstellar dust grains. In DDA an arbitrarily shaped particle is treated as a three dimensional assembly of dipoles on a cubic grid. Each dipole cell is assigned a complex polarizability which can be computed from the complex refractive index of the bulk material and the number of dipoles in a unit volume. The dipoles of course interact with one another via their electric fields, [31, 32] so the DDA is also sometimes referred to as the coupled dipole approximation [33, 34] The theoretical basis for the DDA, including radiative reaction corrections, is summarized by Draine [35]. The polarizability of each dipole causes an oscillating dipole moment or polarization $\boldsymbol{P}_i$ at each cell, depending on the total electric field at the respective position:

$$\boldsymbol{P}_i = \alpha_i \boldsymbol{E}_i \tag{12}$$

The total field $\boldsymbol{E}_i$ is the sum of the incident field $\boldsymbol{E}_{inc,i}$ and the contribution from all other dipoles:

$$\boldsymbol{E}_{\text{other},i} = -\sum_{i \neq j} \boldsymbol{A}_{ij} \boldsymbol{P}_j \tag{13}$$

$$(\alpha_1)^{-1} \boldsymbol{P}_j + \sum_{i \neq j} \boldsymbol{A}_{ij} \boldsymbol{P}_j = \boldsymbol{E}_{\text{inc},i} \tag{14}$$
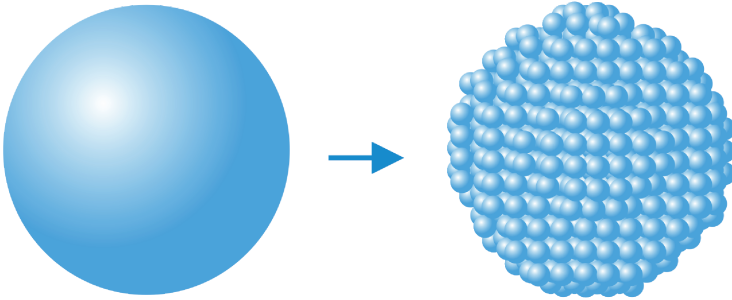

Figure 3. Visualization of the sphere replaced by assembly of dipoles

The matrix $\boldsymbol{A}_{ij}$ includes interaction of all dipoles depending on the distance of the dipoles, thus a full dense matrix results. Beginning with an initial guess of $\boldsymbol{P}_i$, a convergent solution can be obtained. The incident field is a plane wave. This equation can be solved by iteration. The DDA has been applied to compute scattering by aggregated spheres. The standard check of the accuracy of any DDA model is a comparison with results from Mie theory. The agreement between DDA and Mie theory is very good. Several computer implementations of the DDA method have been compared in terms of their accuracy, speed and usability [36, 37]. Over the recent years, with constantly growing computational capabilities, the discrete dipole approximation has become a powerful method for computing electromagnetic scattering by arbitrarily shaped bodies.

6. Conclusions

Not all, but just a few theories have been reviewed here, with references to more detailed papers. Each theory has its own range of applicability, strong and weak points. It mainly depends on the particle shape, its composition and refractive index and its size relative to the wavelength of the incident wave. Obviously, a single theory will not cover all possible scattering particles and problems of application. When choosing a scattering method for a specific optical particle sizing problem, one should also consider the demands of the respective method in terms of computer resources, computer memory and execution time, in addition to the parameters of the method in question that govern the accuracy of the final computational results. A surface-based method will need less computer memory than a volume-based method for the same size of the scatterer. Hence, scattering by larger particles can be computed with surface-based methods. Numerical light scattering modeling is progressing rapidly especially with fast advancing research fields such as nanophotonics and near-field optics.

References

[1] Wriedt T 1998 *Particle & Particle Systems Characterization* **15** (2) 67
[2] Kahnert F M 2003 *Journal of Quantitative Spectroscopy and Radiative Transfer* **79** 775
[3] Veronis G and Fan S 2007 *Springer series in optical sciences* **131** 169
[4] Myroshnychenko V, Rodríguez-Fernández J, Pastoriza-Santos I, Funston A M, Novo C, Mulvaney P, Liz-Marzán L M and Abajo F J G de 2008 *Chemical Society Reviews* **37** (9) 1792
[5] Veselago V, Braginsky L, Shklover V and Hafner C 2006 *Journal of Computational and Theoretical Nanoscience* **3** (2) 189
[6] Mie G 1908 *Annals of Physics* **25** 376
[7] Born M and Wolf E 1975 *Principles of Optics*, *Pergamon*
[8] Bohren C F and Huffmann D R 1983 *Absorption and scattering of light by small particles*, *Wiley-Interscience*
[9] Siu G G and Cheng L 2002 *Journal of the Optical Society of America B* **19** (8) 1922
[10] Du H 2004 *Applied Optics* **43** (9) 1951
[11] Shen J and Cai X 2005 *PIERS Online* **1** (6) 691
[12] Toon O B and Ackerman T P 1981 *Applied Optics* **20** (20) 3657
[13] Kaiser T and Schweiger G 1993 *Computers in Physics* **7** (6) 682
[14] Pieri L A De, Ludlow I K and Waites W M 1993 *The Journal of applied bacteriology* **74** (5) 578
[15] Kreibig U and Vollmer M 1995 *Optical Properties of Metal Clusters (Springer Series in Material Science)*, *Springer* **25**
[16] Shopa M, Kolwas K, Derkachova A and Derkachov G 2010 *Opto-Electronics Review* **18** (4) 421
[17] Kreibig U 2008 *Applied Physics B* **93** (1) 79
[18] Mishchenko M, Videen G, Babenko V, Khlebtsov N and Wriedt T 2004 *Journal of Quantitative Spectroscopy and Radiative Transfer* **88** (1-3) 357
[19] Mishchenko M, Videen G, Babenko V, Khlebtsov N and Wriedt T 2007 *Journal of Quantitative Spectroscopy and Radiative Transfer* **106** (1) 304
[20] Waterman P, Mishchenko M, Travis L and Mackowski D 2015 *Astrophysics Source Code Library* **1** 11006
[21] Yee K S *et al.* 1966 *IEEE Transactions on Antennas and Propagation* **14** (3) 302

[22] Grosges T, Vial A and Barchiesi D 2005 *Optics Express* **13** (21) 8483

[23] Taflove A, Oskooi A and Johnson S 2013 *Artech house*

[24] Schneider J 1995 *IEEE Antennas and Propagation Magazine* **37** (4) 39

[25] BigBoy   *sourceforge.net/projects/bigboy/* [Online; accessed 20-February-2016]

[26] Meep   *ab-initio.mit.edu/wiki/index.php/Main_Page* [Online; accessed 20-February-2016]

[27] GMES   *gmes.sourceforge.net/* [Online; accessed 20-February-2016]

[28] GEMS   *www.2comu.com/products_software_package.html* [Online; accessed 20-February-2016]

[29] DeVoe H 1964 *The Journal of chemical physics* **41** (2) 393

[30] DeVoe H 1965 *The Journal of chemical physics* **43** (9) 3199

[31] Purcell E M and Pennypacker C R 1973 *Astrophysics Journal* **186** 705

[32] Draine B T 1988 *The discrete-dipole approximation and its application to interstellar graphite grains*, *Astrophysics Journal* **333** 848

[33] Singham S B and Salzman G C 1986 *The Journal of Chemical Physics* **84** (5) 2658

[34] Singham S B and Bohren C F 1987 *Optics Letters* **12** (1) 10

[35] Draine B T and Flatau P J 1994 *Journal of the Optical Society of America A* **11** (4) 1491

[36] Penttilä A, Zubko E, Lumme K, Muinonen K, Yurkin M, Draine B, Rahola J, Hoekstra A and Shkuratov Y 2007 *Journal of Quantitative Spectroscopy and Radiative Transfer* **106** (1) 417

[37] Sabouroux P, Stout B, Geffrin J M, Eyraud C, Ayranci I, Vaillon R and Selçuk N 2007 *Journal of Quantitative Spectroscopy and Radiative Transfer* **103** (1) 156